Travelling-wave spatially periodic forcing of asymmetric binary mixtures

Lennon Ó Náraigh

Home fixture

8th October 2018

Context of work I

- Binary alloys phase separate below a critical temperature. The same phenomenon occurs for a wide range of mixtures.
- A mathematical model (first introduced for the binary alloys) for phase separation is the Cahn–Hilliard equation:

$$\frac{\partial c}{\partial t} = D\nabla^2 \left(c^3 - c - \gamma \nabla^2 c\right)$$

where c is the concentration field, D is the diffusion coefficient and $\sqrt{\gamma}$ is a length.

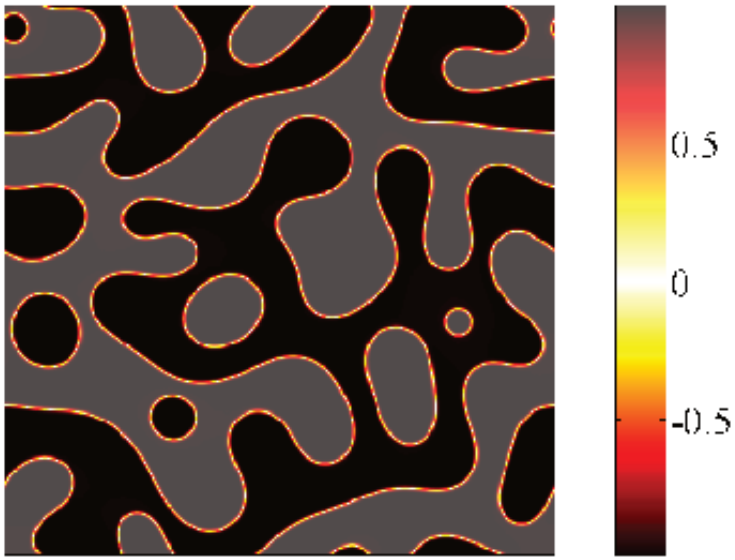

The solution is $c = \pm 1$ in domains with transition regions of thickness $\sqrt{\gamma}$ in between. The domains grow in time. The constant solution $c = 0$ is a well-mixed state but it is unstable.

The values $c = \pm 1$ are energetically favourable.

Context of work II

- There are many ways to control the phase separation.
- We look at a travelling-wave **forcing term** in one spatial dimension:

$$\frac{\partial c}{\partial t} = D\frac{\partial^2}{\partial x^2}\left(c^3 - c - \gamma\frac{\partial^2 c}{\partial x^2}\right) + f_0 k\cos[k(x - vt)], \qquad x \in (-\infty, \infty).$$

  where f_0 is the forcing amplitude, etc.
- With appropriate boundary conditions, the forcing term is consistent with the conservation of the spatial mean concentration,

$$\frac{\partial}{\partial t}\int_{-\infty}^{\infty} c(x,t)\,\mathrm{d}x = 0.$$

Preliminaries I

- We seek travelling-wave **periodic** solutions of the forced Cahn–Hilliard equaiton,

$$c(x,t) = \psi(\eta), \qquad \eta = x - vt, \qquad \psi(\eta + L) = \psi(\eta), \qquad L = 2\pi/k.$$

- As such, we seek solutions of the ODE

$$-\frac{\mathrm{d}\psi}{\mathrm{d}\eta} = D\frac{\mathrm{d}^2}{\mathrm{d}\eta^2}\left(\psi^3 - \psi - \gamma\frac{\mathrm{d}^2\psi}{\mathrm{d}\eta^2}\right) + f_0 k\cos(k\eta).$$

- We can integrate once to reduce the order. After eliminating constants of integration, we get

$$\gamma D\frac{\mathrm{d}^3\psi}{\mathrm{d}\eta^3} = D\frac{\mathrm{d}}{\mathrm{d}\psi}(\psi^3 - \psi) + v(\psi - \langle\psi\rangle) + f_0\sin(k\eta), \tag{1}$$

Spatial average: $\langle\psi\rangle = L^{-1}\int_0^L \psi(\eta)\,\mathrm{d}\eta$.

The aim of the talk is to characterize the solutions of Equation (1).

Preliminaries II

Motivated by applications, we can take $\epsilon = \gamma/L \to 0$. We attempt a regular perturbation theory, with $\psi(\eta) = \psi_0(\eta) + \epsilon\psi_1(\eta) + \cdots$. This quickly gives us two important scenarios:

Preliminaries II

Motivated by applications, we can take $\epsilon = \gamma/L \to 0$. We attempt a regular perturbation theory, with $\psi(\eta) = \psi_0(\eta) + \epsilon\psi_1(\eta) + \cdots$. This quickly gives us two important scenarios:

1. **The regular limit:** The regular perturbation theory is valid, and we solve

$$0 = D\frac{\mathrm{d}}{\mathrm{d}\psi}(\psi^3 - \psi) + v(\psi - \langle\psi\rangle) + f_0 \sin(k\eta),$$

   i.e. a first-order inhomogeneous ODE (**reduced-order model**).
2. **The singular limit** applies when the regular perturbation theory breaks down. The singular limit requires an examination of the ODE (1) with higher derivatives (**the full model**).

Preliminaries II

Motivated by applications, we can take $\epsilon = \gamma/L \to 0$. We attempt a regular perturbation theory, with $\psi(\eta) = \psi_0(\eta) + \epsilon\psi_1(\eta) + \cdots$. This quickly gives us two important scenarios:

1. **The regular limit:** The regular perturbation theory is valid, and we solve

$$0 = D\frac{\mathrm{d}}{\mathrm{d}\psi}(\psi^3 - \psi) + v(\psi - \langle\psi\rangle) + f_0 \sin(k\eta),$$

   i.e. a first-order inhomogeneous ODE (**reduced-order model**).
2. **The singular limit** applies when the regular perturbation theory breaks down. The singular limit requires an examination of the ODE (1) with higher derivatives (**the full model**).

Important solution: When $f_0 = v = 0$, we have the following special solution of the full model:

$$\psi(\eta) = \tanh\left(\frac{\eta - \eta_0}{\sqrt{\gamma}}\right).$$

Knowing this will later on help us to characterize the singular limit (full model) with f_0 and v nonzero, but with $\epsilon \to 0$.

Reduced-order model – first insights I

We look again at the reduced-order model (subscript '0' suppressed):

$$D\frac{\mathrm{d}\psi}{\mathrm{d}\eta} = -\frac{v(\psi - \langle\psi\rangle)}{3\psi^2 - 1} - \frac{f_0}{3\psi^2 - 1}\sin(k\eta).$$

- We have $\psi_{\mathsf{max/min}}$ at $\mathrm{d}\psi/\mathrm{d}\eta = 0$, hence

$$\psi_{\mathsf{max/min}} = \langle\psi\rangle - \frac{f_0}{v}\sin(k\eta_{\mathsf{max/min}}).$$

Reduced-order model – first insights I

We look again at the reduced-order model (subscript '0' suppressed):

$$D\frac{\mathrm{d}\psi}{\mathrm{d}\eta} = -\frac{v(\psi - \langle\psi\rangle)}{3\psi^2 - 1} - \frac{f_0}{3\psi^2 - 1}\sin(k\eta).$$

- We have $\psi_{\mathsf{max/min}}$ at $\mathrm{d}\psi/\mathrm{d}\eta = 0$, hence

$$\psi_{\mathsf{max/min}} = \langle\psi\rangle - \frac{f_0}{v}\sin(k\eta_{\mathsf{max/min}}).$$

- But for this to make sense, the apparent singluarity at $3\psi^2 - 1 = 0$ can never be reached.
- Places constraints on the parameters $\langle\psi\rangle$, v, and f_0:

Case 0:	$1/\sqrt{3} < \langle\psi\rangle - (f_0/v)$,
Case 1:	$\langle\psi\rangle - (f_0/v) > -1/\sqrt{3}$ and $\langle\psi\rangle + (f_0/v) < 1/\sqrt{3}$,
Case 2:	$\langle\psi\rangle + (f_0/v) < -1/\sqrt{3}$.

Sufficient conditions for validity of reduced-order model.

Reduced-order model – first insights II

To find **necessary conditions** we solve the reduced-order model numerically.

- Rather, we solve for $X = \psi^3 - \psi$:

$$D\frac{\mathrm{d}X}{\mathrm{d}\eta} + v\left(\psi_j(X) - \langle\psi\rangle\right) + f_0\sin(k\eta) = 0, \qquad X(L) = X(0),$$

where ψ_j solves $\psi_j^3 - \psi_j = X$, $j = 0, 1, 2$ (roots of cubic), i.e.

$$\psi_j = \frac{2}{\sqrt{3}}\cos\left[\tfrac{1}{3}\cos^{-1}\left(\tfrac{3\sqrt{3}}{2}X\right) - \tfrac{2\pi j}{3}\right], \qquad j = 0, 1, 2.$$

- Real solution of X (hence, ψ_j) indicates validity of reduced-order model, whereas...
- Complex solution of X indicates cusp in ψ_j, hence breakdown of derivative in $\mathrm{d}\psi/\mathrm{d}\eta = \cdots$

Reduced-order model – parameter space

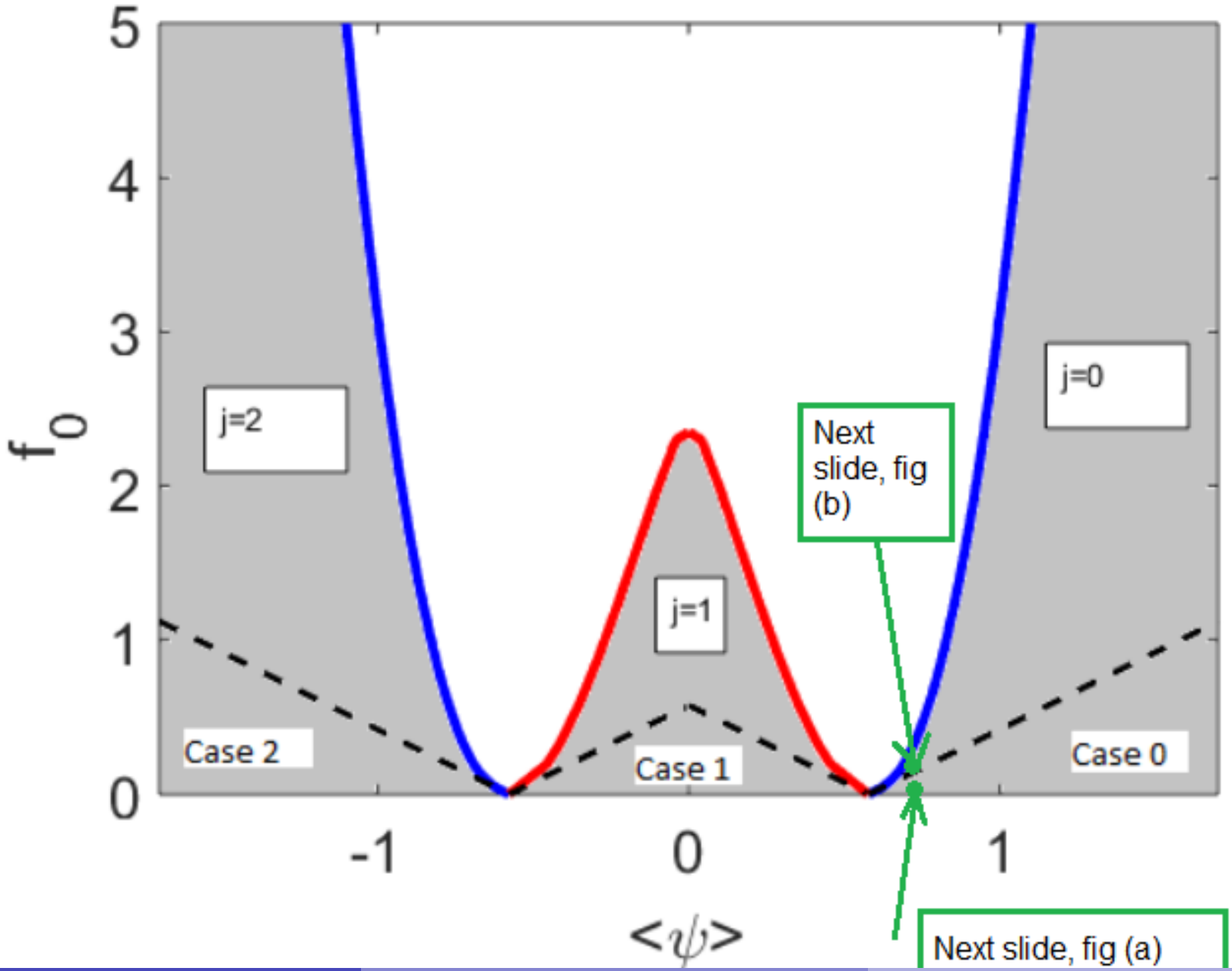

The white area in the parameter space indicates a breakdown of the reduced-order model

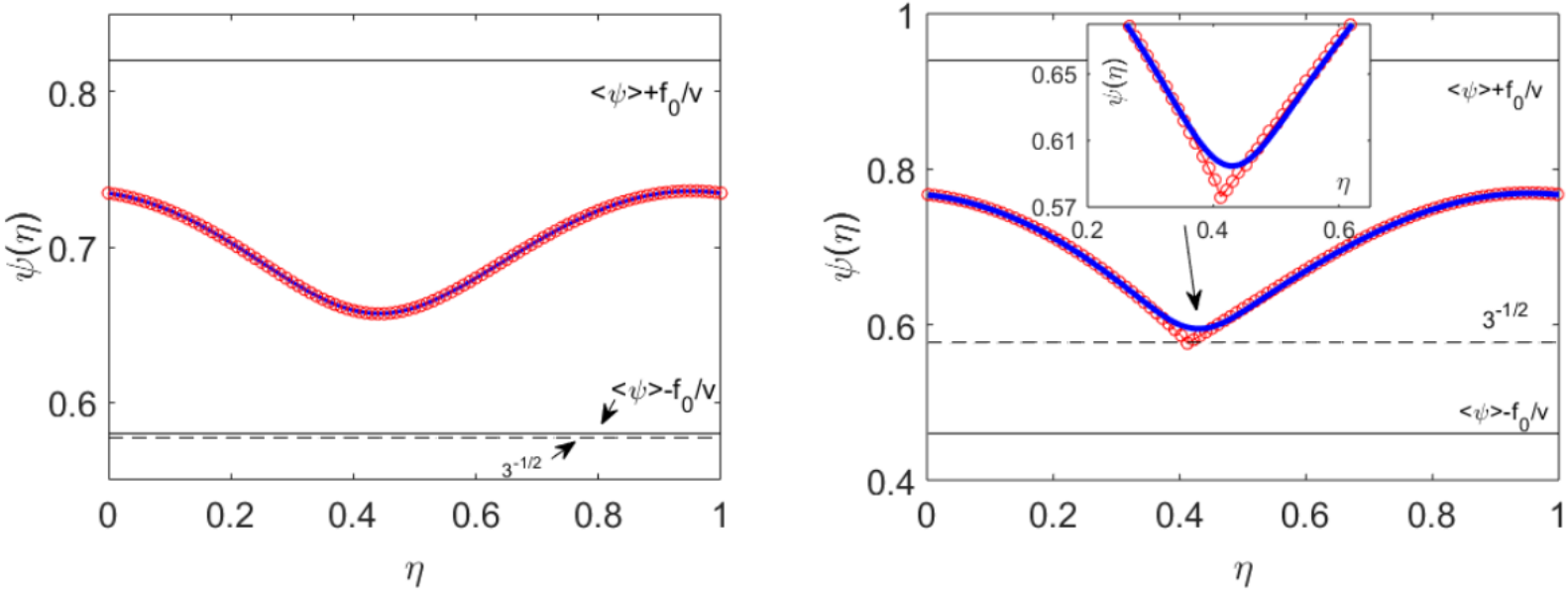

(a) $f_0 = 0.12$ (b) $f_0 = 0.24$

Sample L-periodic numerical solutions of the full model (Equation (5), solid line, with $\epsilon = 10^{-4}$) and the reduced-order model (Equation (7), circles). The following parameters are the same in both panels: $\langle\psi\rangle = 0.7$, $v = D = L = 1$, $k = 2\pi$. The inset in panel (b) is an enlargement of the main figure which shows the formation of the cusp in more detail. Details of the numerical method are provided below at the foot of this section (Section II) and also in A.

Reduced-order model – Rigorous theoretical analysis

- Although the figure explains everything, it is not rigorous.

Reduced-order model – Rigorous theoretical analysis

- Although the figure explains everything, it is not rigorous.
- We can prove rigorous results in the subcases, e.g. **Case 1**, with initial conditions in the range

$$I = [a, b] = [\langle\psi\rangle - (f_0/v), \langle\psi\rangle + (f_0/v)].$$

Reduced-order model – Rigorous theoretical analysis

- Although the figure explains everything, it is not rigorous.
- We can prove rigorous results in the subcases, e.g. **Case 1**, with initial conditions in the range

$$I = [a, b] = [\langle\psi\rangle - (f_0/v), \langle\psi\rangle + (f_0/v)].$$

- We construct a map $f : I \to \mathbb{R}$ that takes initial conditions ($\eta = 0$) in I to final conditions at $\eta = L$. Only some of these initial/final conditions lead to periodic solutions.

Reduced-order model – Rigorous theoretical analysis

- Although the figure explains everything, it is not rigorous.
- We can prove rigorous results in the subcases, e.g. **Case 1**, with initial conditions in the range

$$I = [a, b] = [\langle\psi\rangle - (f_0/v), \langle\psi\rangle + (f_0/v)].$$

- We construct a map $f : I \to \mathbb{R}$ that takes initial conditions ($\eta = 0$) in I to final conditions at $\eta = L$. Only some of these initial/final conditions lead to periodic solutions.
- Periodic solutions of the reduced-order model correspond to fixed points of the map, i.e. $f(\psi_*) = \psi_*$ corresponds to a periodic solution $\psi(\eta + L) = \psi(\eta)$, with $\psi(0) = \psi(L) = \psi_*$.

Reduced-order model – Rigorous theoretical analysis I

- The construction of the map is facilitated by looking at the inhomogeneous reduced-order ODE as a 2D dynamical system:

$$\frac{\mathrm{d}}{\mathrm{d}\eta}\begin{pmatrix} z \\ \psi \end{pmatrix} = \begin{pmatrix} 1 \\ -\mathcal{R}(3\psi^2 - 1, \delta)\left[v(\psi - \langle\psi\rangle) + f_0 \sin(kz)\right] \end{pmatrix},$$

  with initial conditions

$$z = 0, \qquad \psi = \psi_0 \qquad \text{at } \eta = 0.$$

- Here, $\mathcal{R}$ is a regularization:

$$\mathcal{R}(s, \delta) = \frac{s}{s^2 + \delta^2}, \qquad \mathcal{R} \sim 1/s \text{ for } s \to 0 \text{ with } \delta \neq 0.$$

- It will be helpful to write the dynamical system in a more compact form as follows:

$$\frac{\mathrm{d}}{\mathrm{d}\eta}\begin{pmatrix} z \\ \psi \end{pmatrix} = \begin{pmatrix} 1 \\ F_\delta(\psi, z) \end{pmatrix}.$$

Reduced-order model – Rigorous theoretical analysis II

- The dynamical system has no fixed points, limit cycles, ... Hence, $f : I \to J$, where $f(I) = J$ is another interval now (and not some weird set...).

Reduced-order model – Rigorous theoretical analysis II

- The dynamical system has no fixed points, limit cycles, ... Hence, $f : I \to J$, where $f(I) = J$ is another interval now (and not some weird set...).
- Only dynamically important feature is the nullcline $\psi = \langle\psi\rangle - (f_0/v)\sin(k\eta)$.

Reduced-order model – Rigorous theoretical analysis II

- The dynamical system has no fixed points, limit cycles, ... Hence, $f : I \to J$, where $f(I) = J$ is another interval now (and not some weird set...).
- Only dynamically important feature is the nullcline $\psi = \langle\psi\rangle - (f_0/v)\sin(k\eta)$.
- Introduce $g(x) = f(x) - x$. Along with the fact that the nullcline can't go below a or above b, this means:
  - A trajectory starting at a will be nonincreasing – $g(a) \leq 0$.
  - A trajectory starting at b will be nondecreasing – $g(b) \geq 0$.

Reduced-order model – Rigorous theoretical analysis II

- The dynamical system has no fixed points, limit cycles, ... Hence, $f : I \to J$, where $f(I) = J$ is another interval now (and not some weird set...).
- Only dynamically important feature is the nullcline $\psi = \langle\psi\rangle - (f_0/v)\sin(k\eta)$.
- Introduce $g(x) = f(x) - x$. Along with the fact that the nullcline can't go below a or above b, this means:
  - A trajectory starting at a will be nonincreasing – $g(a) \leq 0$.
  - A trajectory starting at b will be nondecreasing – $g(b) \geq 0$.
- Hence, $J = f(I)$, and $I \subset J$ (J is the larger set).

Reduced-order model – Rigorous theoretical analysis II

- The dynamical system has no fixed points, limit cycles, ... Hence, $f : I \to J$, where $f(I) = J$ is another interval now (and not some weird set...).
- Only dynamically important feature is the nullcline $\psi = \langle\psi\rangle - (f_0/v)\sin(k\eta)$.
- Introduce $g(x) = f(x) - x$. Along with the fact that the nullcline can't go below a or above b, this means:
  - A trajectory starting at a will be nonincreasing – $g(a) \leq 0$.
  - A trajectory starting at b will be nondecreasing – $g(b) \geq 0$.
- Hence, $J = f(I)$, and $I \subset J$ (J is the larger set).
- By continuity of g there is at least one zero, $g(x_*) = 0$, hence $f(x_*) = x_*$, hence fixed point exists.

Reduced-order model – Rigorous theoretical analysis II

- The dynamical system has no fixed points, limit cycles, ... Hence, $f : I \to J$, where $f(I) = J$ is another interval now (and not some weird set...).
- Only dynamically important feature is the nullcline $\psi = \langle\psi\rangle - (f_0/v)\sin(k\eta)$.
- Introduce $g(x) = f(x) - x$. Along with the fact that the nullcline can't go below a or above b, this means:
  - A trajectory starting at a will be nonincreasing – $g(a) \leq 0$.
  - A trajectory starting at b will be nondecreasing – $g(b) \geq 0$.
- Hence, $J = f(I)$, and $I \subset J$ (J is the larger set).
- By continuity of g there is at least one zero, $g(x_*) = 0$, hence $f(x_*) = x_*$, hence fixed point exists.
- As we have now found a regular periodic solution with $x_* \in I$ (and nowhere near the singularity at $\pm 1/\sqrt{3}$ we can now safely take $\delta \to 0$ in the regularization $\mathcal{R}(3\psi^2 - 1, \delta)$.

A graphical description of the proof

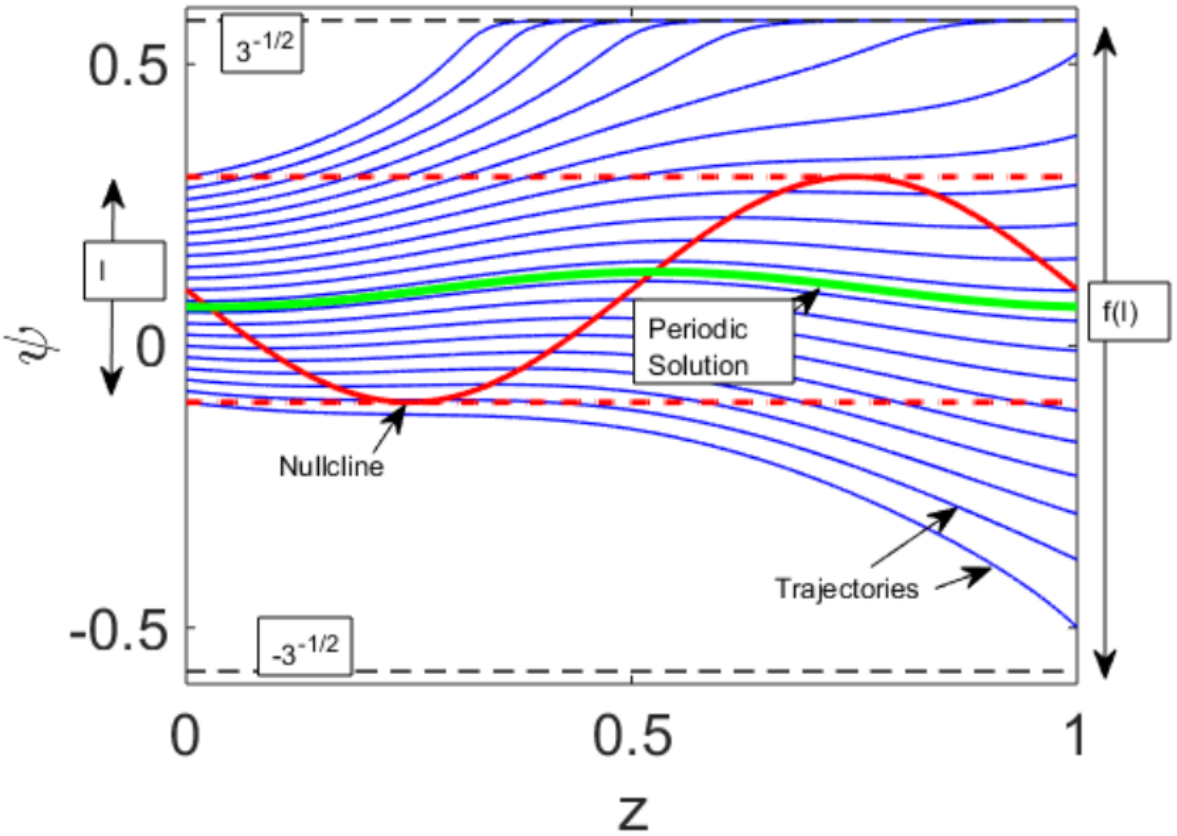

The construction of the f-function mapping the interval I to $[-1/\sqrt{(3)}, 1/\sqrt{3}]$ (Case 1). Shown also is the nullcline $\psi = \langle\psi\rangle - (f_0/v)\sin(kz)$ across which $\mathrm{d}\psi/\mathrm{d}\eta$ changes sign.

Aside – Brouwer's Fixed Point Theorem

- The above is a special (very simple) case of Brouwer's Fixed Point Theorem:

> If $f : X \mapsto X$ is a continuous map from a compact convex X set to itself, then f has at least one fixed point.

- Fluid mechanics application: Put a fluid in a convex container (the fluid completely fills the container), and stir the fluid for a period of time T. Then there is at least one fluid particle that ends up where it started.

Reduced-order model – Uniqueness of Fixed Points

From the numerics we 'know' that the periodic solutions are unique. We can also prove this rigorously in certain cases. We use:

$$|f(\psi_1) - f(\psi_0)| \leq \max_{x \in I} |f'(x)||\psi_1 - \psi_0|.$$

- If $\max_{x \in I} |f'(x)| < 1$ for all $x \in I$ the map $f : I \to J$ is a contraction mapping.
- If $\max_{x \in I} |f'(x)| > 1$ for all $x \in I$ the inverse map $f^{-1} : J \to I$ is a contraction mapping.

In either case, **Banach's fixed point theorem** then establishes that the already-derived fixed point (i.e. periodic solution) is unique.

Therefore, to make progress with uniqueness, we need to be able to evaluate $f'(x)$.

To evaluate $f'(x)$ we need to know about the flow.

Recall, the map f maps an initial condition ψ_0 to a final condition $\psi(\eta = L)$.
This can be connected to the flow of the (regularized) 2D dynamical system.

- The 2D dynamical system is recalled here as

$$\frac{\mathrm{d}}{\mathrm{d}\eta}\begin{pmatrix} z \\ \psi \end{pmatrix} = \begin{pmatrix} 1 \\ F_\delta(\psi, z) \end{pmatrix}.$$

- The corresponding flow is

$$\begin{aligned} \varphi_\delta : \mathbb{R}^2 \times \mathbb{R} &\to \mathbb{R}^2, \\ ((z_0, \psi_0), \eta) &\mapsto \varphi_\delta(z_0, \psi_0, \eta), \end{aligned}$$

(we take $z_0 = 0$).

To evaluate $f'(x)$ we need to know about the flow.

Recall, the map f maps an initial condition ψ_0 to a final condition $\psi(\eta = L)$.
This can be connected to the flow of the (regularized) 2D dynamical system.

- The 2D dynamical system is recalled here as

$$\frac{\mathrm{d}}{\mathrm{d}\eta}\begin{pmatrix} z \\ \psi \end{pmatrix} = \begin{pmatrix} 1 \\ F_\delta(\psi, z) \end{pmatrix}.$$

- The corresponding flow is

$$\begin{aligned} \varphi_\delta : \mathbb{R}^2 \times \mathbb{R} &\to \mathbb{R}^2, \\ ((z_0, \psi_0), \eta) &\mapsto \varphi_\delta(z_0, \psi_0, \eta), \end{aligned}$$

  (we take $z_0 = 0$).

In other words, the flow evolves a solution from the starting time $z = z_0$ to a later time $z + z_0 + \eta$ (we take $z_0 = 0$):

$$\varphi_\delta(0, \psi_0, \eta) = \begin{pmatrix} z = z_0 + \eta \\ \psi(\eta) \end{pmatrix}.$$

Hence,

$$f(\psi_0) = \begin{pmatrix} 0 & 0 \\ 0 & 1 \end{pmatrix} \varphi_\delta(0, \psi_0, L).$$

In Case 1 we get an expansion map $\implies$ unique solution

Using standard results from dynamical systems theory, we can now compute $f'(\psi_0)$:

$$f'(\psi_0) = \exp\left(\int_0^L \frac{\partial F_\delta}{\partial \psi} \mathrm{d}\eta\right).$$

- We can now safely take $\delta \to 0$, as we are evaluating along a regular periodic trajectory.
- Therefore, the sign of $\partial F/\partial \psi$ determines if f' is positive or negative and hence, if we have a contraction / expansion map.
- We compute

$$\frac{\partial F}{\partial \psi} = \frac{3v\psi^2 - 6\psi\left[v\langle\psi\rangle - f_0 \sin(kz)\right] + v}{(3\psi^2 - 1)^2}.$$

In **Case 1** it is possible to show using straightforward algebraic manipulation that $\partial F/\partial \psi > 0$. Hence, f is an expansion map so f^{-1} is a contraction map and by Banach's Fixed Point Theorem the fixed point (periodic solution) is unique.

Linear Stability Analysis

It is of interest to classify the stability of the periodic solutions – look at a perturbation

$$c(x,t) = \psi(\eta) + \delta c(\eta, t), \qquad \eta = x - vt.$$

- Sub into CH equation (full model) and linearize:

$$\frac{\partial}{\partial t}\delta c - v\frac{\partial}{\partial \eta}\delta c = D\frac{\partial^2}{\partial \eta^2}\left(\mathcal{S}\delta c\right) - \gamma\frac{\partial^4}{\partial \eta^4}\delta c, \qquad \mathcal{S} = 3\psi^2 - 1.$$

- Take $\gamma \to 0$ (reduced model).
- Eigenvalue analysis $\delta c = \mathrm{e}^{\lambda t}\widetilde{\delta c}(\eta)$:

$$\lambda\widetilde{\delta c} - v\frac{\partial}{\partial \eta}\widetilde{\delta c} = D\frac{\partial^2}{\partial \eta^2}\left(\mathcal{S}\widetilde{\delta c}\right)$$

- **Boundary conditions** are $\delta c \to 0$ as $|\eta| \to \infty$ (perturbation dies out at infinity).

Linear Stability Analysis I

- The eigenvalue problem is second-order linear with **periodic** coefficients ($\mathcal{S} = 3\psi^2 - 1$ is periodic). Therefore, the eigenfunctions are Bloch waves:

$$\widetilde{\delta c} = \mathrm{e}^{\mathrm{i}p\eta}\Phi_p(\eta), \qquad \Phi_p(\eta + L) = \Phi_p(\eta).$$

- Theory (Kenny, First ACM seminar this semester) tells us that the most unstable mode occurs at $p = 0$. This corresponds to a periodic disturbance. We therefore look at the eigenvalue problem

$$\lambda\Phi_0 - v\frac{\partial\Phi_0}{\partial\eta} = D\frac{\partial^2}{\partial\eta^2}\left(\mathcal{S}\Phi_0\right), \qquad \Phi_0(\eta + L) = \Phi_0(\eta).$$

- By integrating both sides from 0 to η and using the periodic boundary conditions, we see that either $\lambda = 0$ or $\langle\Phi_0\rangle = 0$ (mean zero spatial average).
- In the first case ($\lambda = 0$) there is no instability, so look at second case ($\langle\Phi_0\rangle = 0$).

Linear Stability Analysis II

In the second case ($\langle \Phi_0 \rangle = 0$) we multiply both sides of the eigenvalue problem by Ψ_0^* and integrate. After some IBP, we obtain

$$\mathrm{Re}(\lambda)\|\Phi_0\|_2^2 = -\int_0^L \mathcal{S}|\Phi_0'|^2 + \tfrac{1}{2}\int_0^L \mathcal{S}''|\Phi_0|^2.$$

Linear Stability Analysis II

In the second case ($\langle \Phi_0 \rangle = 0$) we multiply both sides of the eigenvalue problem by Ψ_0^* and integrate. After some IBP, we obtain

$$\mathrm{Re}(\lambda)\|\Phi_0\|_2^2 = -\int_0^L \mathcal{S}|\Phi_0'|^2 + \tfrac{1}{2}\int_0^L \mathcal{S}''|\Phi_0|^2.$$

Hence,

$$\begin{aligned}
\mathrm{Re}\lambda\|\Phi_0\|_2^2 &\leq -\mathcal{S}_{\min}\int_0^L |\Phi_0'|^2 + \tfrac{1}{2}\max|\mathcal{S}''|\int_0^L |\Phi_0|^2, \\
&= -\mathcal{S}_{\min}\|\Phi_0'\|_2^2 + \tfrac{1}{2}\max|\mathcal{S}''|\|\Phi_0\|_2^2, \\
&\overset{\text{Poincaré}}{\leq} -\mathcal{S}_{\min}(2\pi/L)^2\|\Phi_0\|_2^2 + \tfrac{1}{2}\max|\mathcal{S}''|\|\Phi_0\|_2^2,
\end{aligned}$$

where we can use Poincaré's inequality in this neat way because $\langle \Phi_0 \rangle = 0$.

Linear Stability Analysis II

In the second case ($\langle \Phi_0 \rangle = 0$) we multiply both sides of the eigenvalue problem by Ψ_0^* and integrate. After some IBP, we obtain

$$\mathrm{Re}(\lambda)\|\Phi_0\|_2^2 = -\int_0^L \mathcal{S}|\Phi_0'|^2 + \tfrac{1}{2}\int_0^L \mathcal{S}''|\Phi_0|^2.$$

Hence,

$$\begin{aligned}
\mathrm{Re}\lambda\|\Phi_0\|_2^2 &\leq -\mathcal{S}_{\min}\int_0^L |\Phi_0'|^2 + \tfrac{1}{2}\max|\mathcal{S}''|\int_0^L |\Phi_0|^2, \\
&= -\mathcal{S}_{\min}\|\Phi_0'\|_2^2 + \tfrac{1}{2}\max|\mathcal{S}''|\|\Phi_0\|_2^2, \\
&\overset{\text{Poincaré}}{\leq} -\mathcal{S}_{\min}(2\pi/L)^2\|\Phi_0\|_2^2 + \tfrac{1}{2}\max|\mathcal{S}''|\|\Phi_0\|_2^2,
\end{aligned}$$

where we can use Poincaré's inequality in this neat way because $\langle \Phi_0 \rangle = 0$.

Therefore, a sufficient condition for stability is

$$\mathcal{S}_{\min}(2\pi/L)^2 \geq \tfrac{1}{2}\max_{[0,L]}|\mathcal{S}''|.$$

Linear stability – parameter space

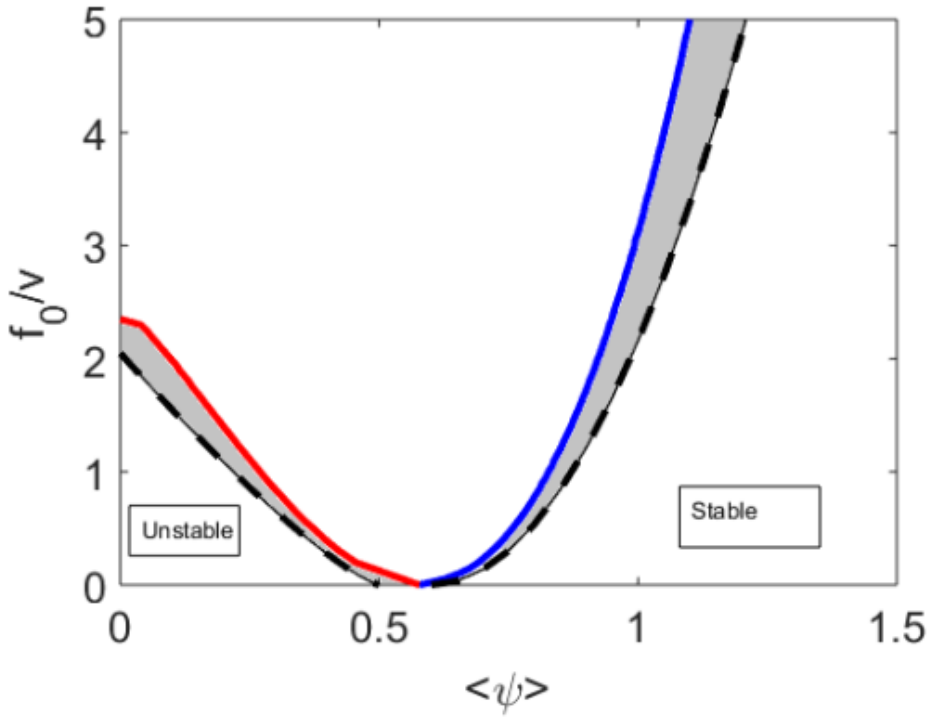

Reduced-order model: Plot of the parameter subspace $(\langle\psi\rangle, f_0)$ at fixed $v = 1$. A large part of Region 0 corresponds to stable travelling waves as indicated. In the remaining part of Region 0 (shaded), the stability of the travelling waves is not known *a priori*. A similar picture holds in Region 1.

The full model

- We look now at the full model – this covers cases where the reduced-order model breaks down.

The full model

- We look now at the full model – this covers cases where the reduced-order model breaks down.
- The full model is recalled here as (with $\gamma \to \epsilon$) corresponding to the small interface width:

$$\epsilon D \frac{\mathrm{d}^3\psi}{\mathrm{d}\eta^3} = D\frac{\mathrm{d}}{\mathrm{d}\eta}\left(\psi^3 - \psi\right) + v\left(\psi - \langle\psi\rangle\right) + f_0 \sin(k\eta). \tag{2}$$

The full model

- We look now at the full model – this covers cases where the reduced-order model breaks down.
- The full model is recalled here as (with $\gamma \to \epsilon$) corresponding to the small interface width:

$$\epsilon D \frac{\mathrm{d}^3\psi}{\mathrm{d}\eta^3} = D\frac{\mathrm{d}}{\mathrm{d}\eta}\left(\psi^3 - \psi\right) + v\left(\psi - \langle\psi\rangle\right) + f_0 \sin(k\eta). \tag{2}$$

- A first approach is to do direct numerical simulations of the corresponding temporally-evolving equation (TENS):

$$\frac{\partial c}{\partial t} - v\frac{\partial c}{\partial \eta} = D\frac{\partial^2}{\partial \eta^2}\left(c^3 - c - \epsilon\frac{\partial^2 c}{\partial \eta^2}\right) + f_0 k\cos(k\eta), \text{ (moving frame).} \tag{3}$$

The full model

- We look now at the full model – this covers cases where the reduced-order model breaks down.
- The full model is recalled here as (with $\gamma \to \epsilon$) corresponding to the small interface width:

$$\epsilon D \frac{\mathrm{d}^3\psi}{\mathrm{d}\eta^3} = D\frac{\mathrm{d}}{\mathrm{d}\eta}\left(\psi^3 - \psi\right) + v\left(\psi - \langle\psi\rangle\right) + f_0 \sin(k\eta). \tag{2}$$

- A first approach is to do direct numerical simulations of the corresponding temporally-evolving equation (TENS):

$$\frac{\partial c}{\partial t} - v\frac{\partial c}{\partial \eta} = D\frac{\partial^2}{\partial \eta^2}\left(c^3 - c - \epsilon\frac{\partial^2 c}{\partial \eta^2}\right) + f_0 k\cos(k\eta), \text{ (moving frame).} \tag{3}$$

- From the TENS (Equation (3)) we look for the emergence of travelling-wave solutions $c(\eta, t) \to \psi(\eta)$ – i.e. solutions of (2).

Two distinct travellling-wave solutions are observed in the full model

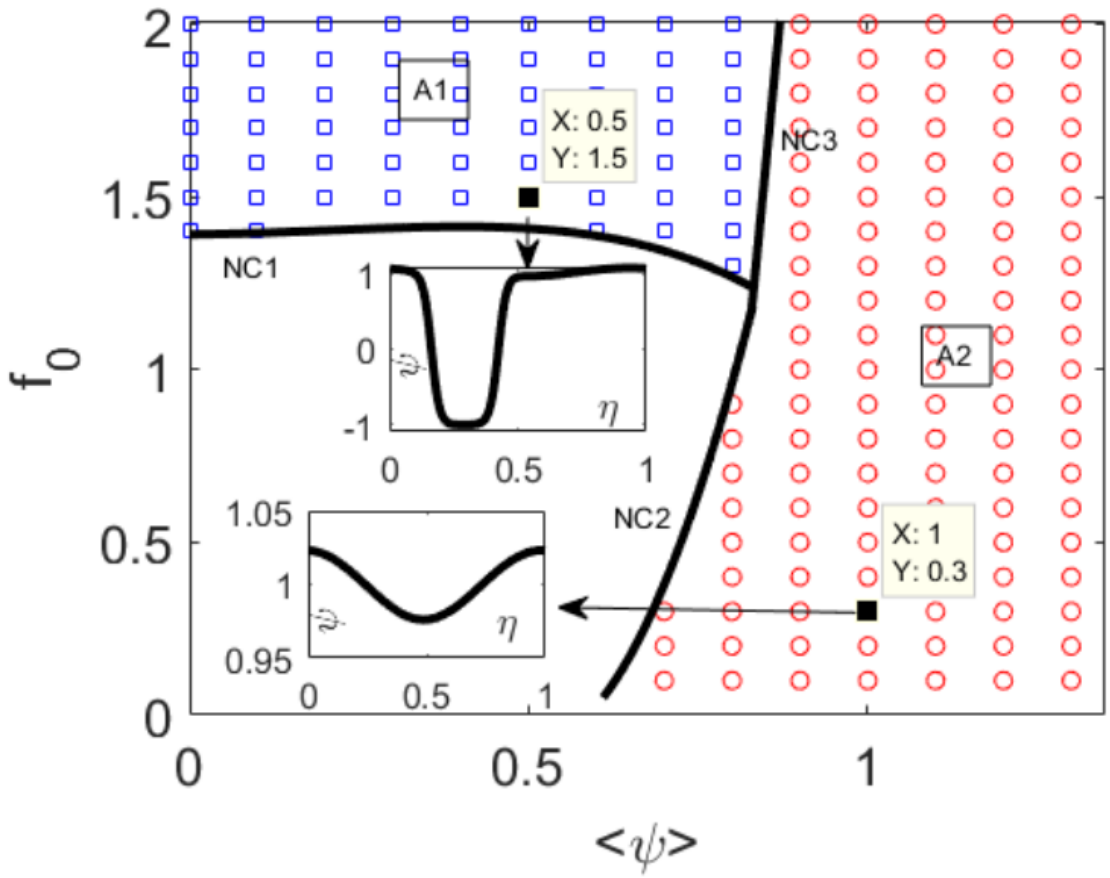

Summary of results of temporally-evolving numerical simulations for fixed $v = 1$, and for various values of $\langle\psi\rangle$ and f_0. Also, the small parameter ϵ is set to 5×10^{-4}. The circles and squares indicate simulations where a steady travelling wave exists.

A1 travelling waves I

- The A2 travelling waves are clearly the same as the stable solutions that appear in the reduced-order
- The A1 travelling waves are new. These can be understood using an intuitive singular perturbation theory, valid as $\epsilon \to 0$.
- This theory back to an idea by **Ted Cox and Dana Mackey**, who used the same approach for forced waves in shallow-water models.

A1 travelling waves II

Recall Equation (2):

$$\epsilon D \frac{\mathrm{d}^3\psi}{\mathrm{d}\eta^3} = D\frac{\mathrm{d}}{\mathrm{d}\eta}\left(\psi^3 - \psi\right) + v\left(\psi - \langle\psi\rangle\right) + f_0 \sin(k\eta).$$

- The spatial variations separate into rapid variations on the scale $\epsilon^{1/2}$ and slow variations on the scale L.

A1 travelling waves II

Recall Equation (2):

$$\epsilon D \frac{\mathrm{d}^3\psi}{\mathrm{d}\eta^3} = D\frac{\mathrm{d}}{\mathrm{d}\eta}\left(\psi^3 - \psi\right) + v\left(\psi - \langle\psi\rangle\right) + f_0 \sin(k\eta).$$

- The spatial variations separate into rapid variations on the scale $\epsilon^{1/2}$ and slow variations on the scale L.
- In the limiting case $v \to 0$ (or $f_0 \to \infty$), the slow variations are governed by the balance

$$D\frac{\mathrm{d}}{\mathrm{d}\eta}(\psi^3 - \psi) \sim f_0 \sin(k\eta),$$

  hence $\psi^3 - \psi \sim -[f_0/(Dk)]\cos(k\eta) + \beta$, where β is a constant of integration.
  - A cubic equation with three possible solutions, parametrized by β.
  - The dynamics select a solution with $\max(\psi) \approx 1$ and $\min(\psi) \approx -1$ because these are energetically favourable in the CH equation.
  - The dynamics further stitch together a patchwork of such solutions.

A1 travelling waves II

Recall Equation (2):

$$\epsilon D \frac{\mathrm{d}^3\psi}{\mathrm{d}\eta^3} = D\frac{\mathrm{d}}{\mathrm{d}\eta}\left(\psi^3 - \psi\right) + v\left(\psi - \langle\psi\rangle\right) + f_0 \sin(k\eta).$$

- The spatial variations separate into rapid variations on the scale $\epsilon^{1/2}$ and slow variations on the scale L.
- In the limiting case $v \to 0$ (or $f_0 \to \infty$), the slow variations are governed by the balance

$$D\frac{\mathrm{d}}{\mathrm{d}\eta}(\psi^3 - \psi) \sim f_0 \sin(k\eta),$$

  hence $\psi^3 - \psi \sim -[f_0/(Dk)]\cos(k\eta) + \beta$, where β is a constant of integration.
  - A cubic equation with three possible solutions, parametrized by β.
  - The dynamics select a solution with $\max(\psi) \approx 1$ and $\min(\psi) \approx -1$ because these are energetically favourable in the CH equation.
  - The dynamics further stitch together a patchwork of such solutions.
- These can be thought of as 'outer solutions' in a singular perturbation theory.

Idea – The outer solutions are stitched together across narrow transition regions

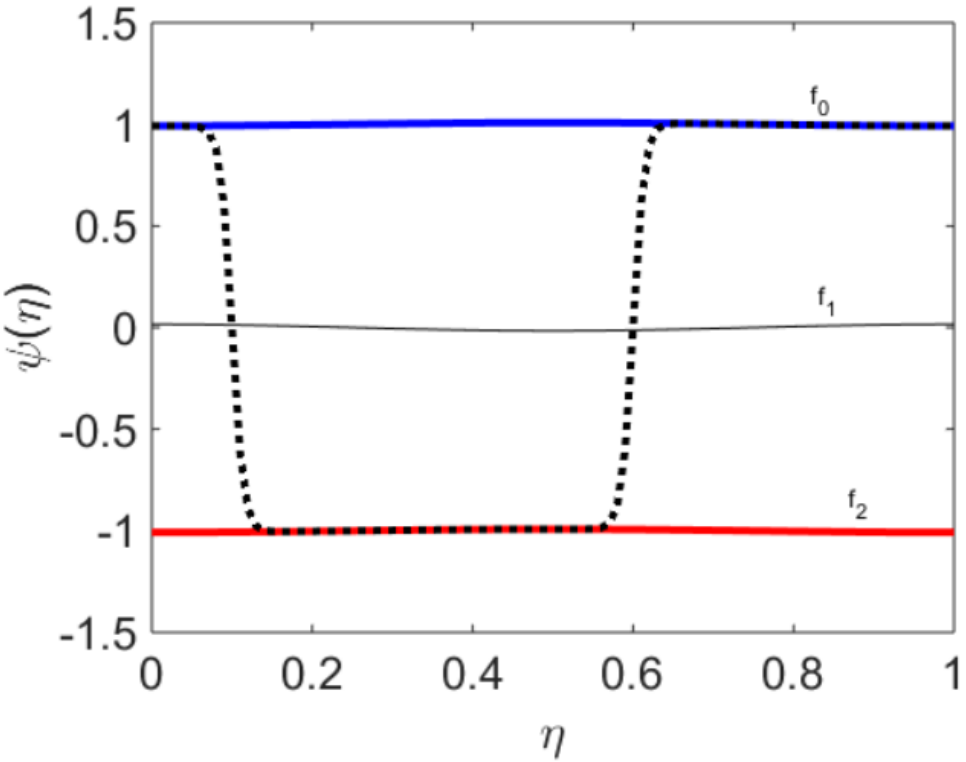

The idea for the construction of the single-spike approximate solution to Equation (39). The approximate solution is constructed by stitching together two f_j-profiles. Recall, the f_j-functions are solution of Equation (40). In this figure, the f_j profiles are joined together across narrow step-like transition regions.

Implementation – The outer solutions are stitched together across narrow transition regions

- Across a small region of width $\epsilon^{1/2}$, distinct outer and inner solutions are patched.
- Here, the dominant balance is

$$\epsilon \frac{\mathrm{d}^3\psi}{\mathrm{d}\eta^3} \sim \frac{\mathrm{d}}{\mathrm{d}\eta}(\psi^3 - \psi)$$

- But the solution of this equation is the special CH solution mentioned earlier – $\tanh$ functions.
- Hence, an **approximate** solution is constructed as

$$\psi^{\text{approx}} = s \tanh\left(\frac{\eta - c_1}{\sqrt{2\epsilon}}\right) \tanh\left(\frac{\eta - c_2}{\sqrt{2\epsilon}}\right), \qquad \epsilon \to 0, \qquad s = 1,$$

where $c_1 = L/4$ and $c_2 = c_1 + (1/2)[L - s\langle\psi\rangle]$ – these choices give

$$\langle\psi^{\text{approx}}\rangle \approx \langle\psi\rangle;$$

the spatial average $\langle\psi\rangle$ is an externally-prescribed parameter.

The Newton solver

The idea now is to use this construction of an approximate solution as a **starting value** in a **Newton solver** for Equation (2), with the understanding that the finite value of v will manifest itself as a simple phase shift between the true solution and ψ^{approx}. This works!

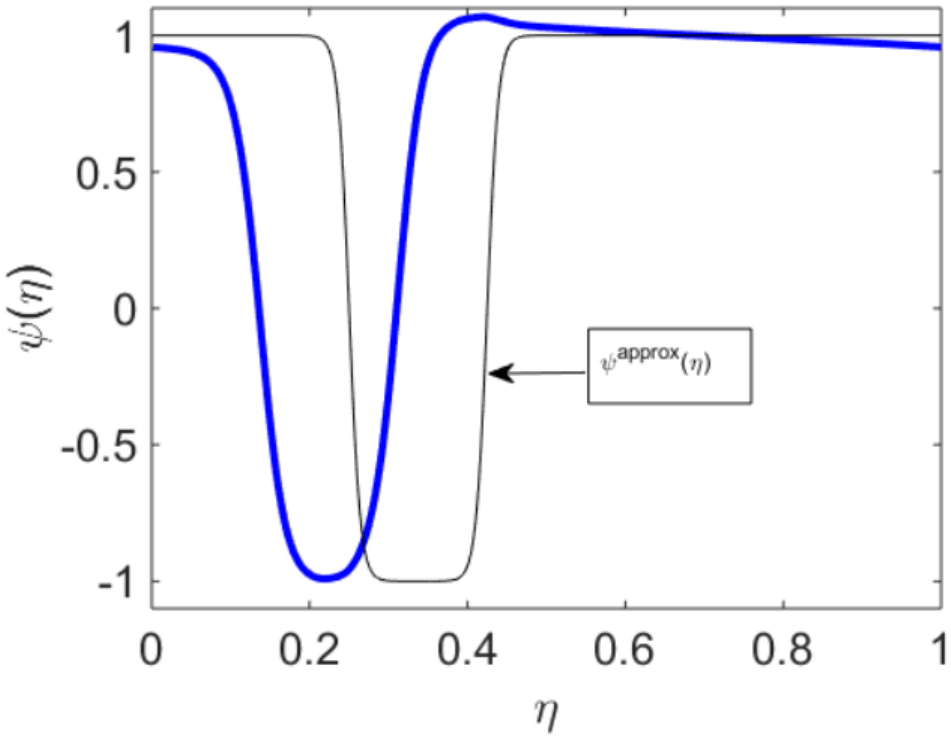

Emergence of single-spike concentration profile from the inital guess $\psi^{\text{approx}}(\eta)$ given by Equation (41). Parameters: $\langle\psi\rangle = 0.65$, $f_0 = 0.1$.

Solutions constructed using the Newton Solver agree with the TENS

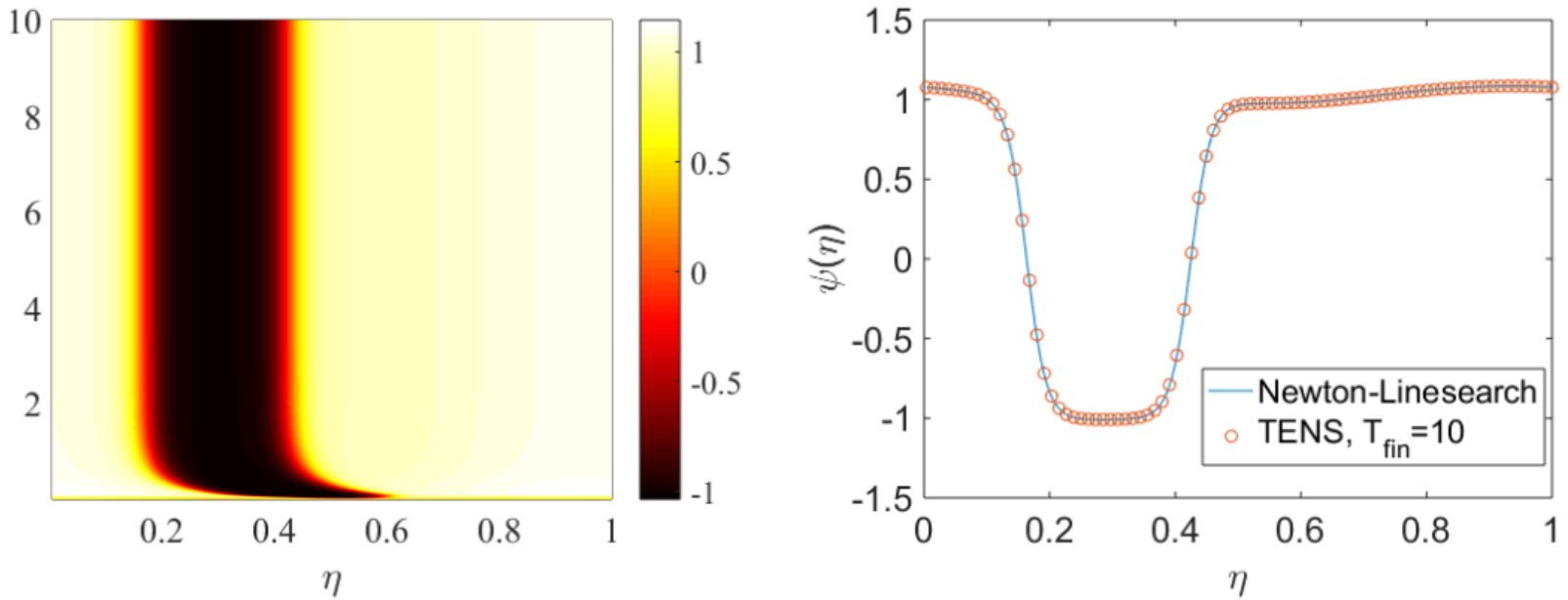

Sample transiently-evolving numerical simulation (TENS) results for the case $\langle\psi\rangle = 0.5$ and $f_0 = 1.5$. Also, $v = 1$, and $\epsilon = 5 \times 10^{-4}$. Panel (a) shows the spacetime evolution of the concentration profile $C(\eta, t)$, up to a final time $T_{\text{fin}} = 10$. Panel (b) shows a snapshot of the concentration at the final time, and a comparison with a steady travelling-wave profile generated with the Newton solver. A timestep $\Delta t = 10^{-4}$ is used. Also, $N = 256$ gridpoints are used in both numerical methods.

Linear stability and multiple-spike solutions

- That the TW solutions constructed with the Newton Solver agree with the TENS is no suprirse.

Linear stability and multiple-spike solutions

- That the TW solutions constructed with the Newton Solver agree with the TENS is no suprirse.
- But this is nice – we can do a linear stability analysis using the solution constructed with the Newton Solver as the base state (equilibrium solution).

Linear stability and multiple-spike solutions

- That the TW solutions constructed with the Newton Solver agree with the TENS is no suprirse.
- But this is nice – we can do a linear stability analysis using the solution constructed with the Newton Solver as the base state (equilibrium solution).
- Linear stability analysis reveals the A1-solution to be stable in the domain shown in the previous parameter space.

Linear stability and multiple-spike solutions

- That the TW solutions constructed with the Newton Solver agree with the TENS is no suprirse.
- But this is nice – we can do a linear stability analysis using the solution constructed with the Newton Solver as the base state (equilibrium solution).
- Linear stability analysis reveals the A1-solution to be stable in the domain shown in the previous parameter space.
- But we can also construct an A2-type solution with $s = -1$ in

$$\psi^{\text{approx}} = s \tanh\left(\frac{\eta - c_1}{\sqrt{2\epsilon}}\right) \tanh\left(\frac{\eta - c_2}{\sqrt{2\epsilon}}\right), \qquad \epsilon \to 0, \qquad s = -1.$$

Linear stability and multiple-spike solutions

- That the TW solutions constructed with the Newton Solver agree with the TENS is no suprirse.
- But this is nice – we can do a linear stability analysis using the solution constructed with the Newton Solver as the base state (equilibrium solution).
- Linear stability analysis reveals the A1-solution to be stable in the domain shown in the previous parameter space.
- But we can also construct an A2-type solution with $s = -1$ in

$$\psi^{\text{approx}} = s \tanh\left(\frac{\eta - c_1}{\sqrt{2\epsilon}}\right) \tanh\left(\frac{\eta - c_2}{\sqrt{2\epsilon}}\right), \qquad \epsilon \to 0, \qquad s = -1.$$

- And there is nothing to stop us from constructing multiple-spike initial guesses:

$$\psi^{\text{approx}} = (\pm 1) \prod_{j=0}^{N} \tanh\left(\frac{N\eta - j - c_1}{\sqrt{2\epsilon}}\right) \tanh\left(\frac{N\eta - j - c_2}{\sqrt{2\epsilon}}\right), \qquad \epsilon \to 0,$$

with c_1 and c_2 unchanged from before.

The Newton Solver produces multiple-spike solutions.

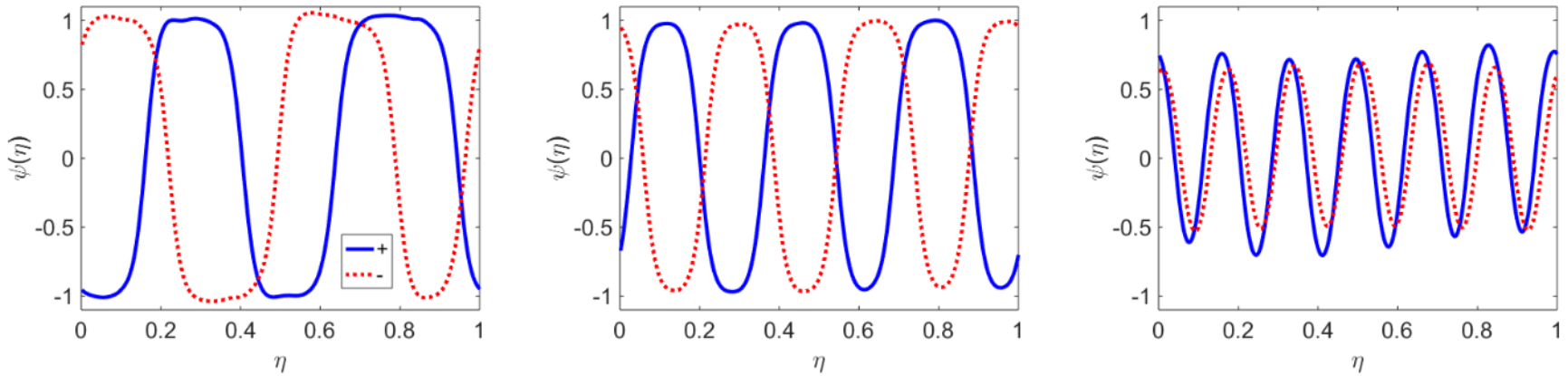

(a) $N = 2$ (b) $N = 3$ (c) $N = 6$

Multiple-spike solutions for $(f_0, v) = (0.1, 1)$ and $\langle\psi\rangle = 0.1$, corresponding to a region in parameter space with no stable travelling waves.

- The multiple-spike solutions are all linearly unstable.
- Cox and Mackey also observed multiple-spike solutions in their work on forced waves in shallow-water models.

Conclusions

- We have rigorously analyzed the travelling-wave solutions of the forced Cahn–Hilliard equation.
- The analysis relies on a range of tools from Dynamical Systems.
- Construction of a zoo of travelling-wave solutions has been accomplished with a Newton solver with a judiciously-chosen initial guess (no time to go into this Newton solver – it is a very sensitive beast – uses a backtracking linesearch to converge on the correct solution).
- The analysis reveals that the mean concentration $\langle \psi \rangle$ and the forcing amplitude f_0 are key parameters that control the shape of the travelling-wave solutions.
- Submitted work:

  https://arxiv.org/abs/1807.08538

- Thanks to Ted Cox for showing me this problem.